Creep behaviour of long fiber PP based composites for the automotive industry

Greco, A. Musardo, C. and Maffezzoli, A.

Dipartimento di Ingegneria dell'Innovazione, Università di Lecce,
via per Monteroni, 73100 Lecce, Italy.
Email: antonio.greco@unile.it

Abstract
In this work the creep behaviour of compression moulded Twintex® sheets has been studied by means of three points flexural tests. Test samples were obtained in a compression moulding apparatus at different temperatures of the mould. Short term flexural creep tests were run at multiple stress levels. The linearity of creep behaviour was tested changing the applied stress and applying the Boltzmann superposition principle. In the linear viscoelastic behaviour region, the temperature was varied between 30 and 152°C. Time-temperature superposition principle was applied to build a master curve, predicting the creep behaviour of the composite at a single reference temperature and long time scales. The behaviour of the composite obtained at different processing conditions was related to the crystalline structures developed in the polymer matrix during processing. Increasing the temperature of the mould resulted in higher degree of crystallinity of the polymer matrix. This was evidenced from x-ray and DSC analysis. In turn, the higher crystalline fraction of the panels moulded at higher temperatures lead to a decrease of tenacity, as evidenced from Charpy impact tests.

Introduction
Fibre reinforced polymer composites are considered as candidate structural materials for lightweight and fuel efficient automobiles of the future. Potential applications of these materials include floor panels, body side frames, cross-members, and front-end structural members. Thermoplastic matrix composites, based on commodity polymers, are attracting a growing interest essentially thanks to their low cost coupled with fast processability, high impact and delamination strength, abrasion and chemical resistance, low moisture absorption, unlimited shelf life of raw materials. In addition, the ability of thermoplastic matrix composites to be recycled is one of the main advantages over thermosetting [1] for the automotive applications. During their service life automobile structures are subjected to creep resulting from constant and cyclic stresses while being exposed to a variety of environments [2]. For a polymer matrix composite subjected to long-term exposure at elevated temperatures, the viscoelastic nature of the polymer matrix can lead to changes in composite stiffness, strength and fatigue life [3]. As a consequence, the creep resulting from sustaining stresses can produce plastic deformation, damage or even failure even for stresses lower than the ultimate strength of the composite [2].
Because of its characteristics of low density, good processability and environmental resistance, isotactic polypropylene (iPP) is considered one of the best thermoplastic candidates for many industrial applications. The low glass transition temperature of PP severely limits its applicability when a long service life at moderate to high temperatures is required. Fibre reinforcing enhances PP mechanical properties, such as stiffness and fracture resistance, and limits the propensity of this material to deform under creep conditions [1].
In this work the flexural creep behaviour of compression moulded Twintex® has been studied. Multiple loading tests were performed to establish the linear viscoelastic (LVE) behaviour region of the composite. The LVE region generally defines the range for the application of polymers as engineering materials [4]. In the LVE region, creep tests were run at different temperatures, and time- temperature superposition principle was used to build master curves, predicting the long-term creep behaviour of the material. Also, Charpy impact tests were performed on compression moulded samples. The effect of processing conditions on the crystalline structure of the matrix,

studied by means of differential scanning calorimetry (DSC) and x-ray analysis, was correlated with the composite creep and impact properties.

Experimental

The material used was Twintex® T PP, woven fabric with commingled E-glass and isotactic polypropylene (iPP) rowings. The material tested is a balanced woven fabric with 60% by weight of glass and 40% by weight iPP. Twintex® T PP fabrics were compression moulded at 20 bar for 10 minutes in a Campana P7-91 hot press. Three plies of Twintex® T PP were bonded, to obtain 1.4mm thick cross-ply laminate with 0° and 90° fiber orientation. The laminates were obtained at different temperatures of the press plates, i.e. 80, 110 and 130°C. The samples obtained at different temperatures have been labelled as sample s80, s110, and s130. Laminates obtained at 80°C were annealed for 1h at 90°C to avoid recrystallization effects during creep tests at high temperature [5]. Rectangular samples (1.4x14x70mm) were cut from the laminate to perform mechanical characterization.

Flexural analysis was performed in the fibre direction. Flexural tests were performed in a Lloyd LR5K instrument with a support span of 60mm. For each test, the sample and the flexural tools were held in the oven for 1h to avoid temperature gradients within the oven and the sample. Static elastic modulus and flexural strength were determined using a crosshead speed of 2mm/min. Creep characterization was performed at different temperatures and stress levels. In each test the crosshead speed during loading of the sample was adjusted as to reach the desired stress level in a time of 5 seconds, as predicted by test standards [6]. The stress was held for 90 minutes, and the displacement of the sample was recorded. Creep experiments were performed at different load levels in order to establish the LVE region of the composite. The load was ranged from 14 to 84% of the break up load determined from static flexural tests. In the LVE region, tests were performed at different temperatures for each sample. Time-temperature superposition principle was applied to build a single master curve at a reference temperature of 30°C.

Charpy impact tests were performed at room temperature in a ATS FAAR model IMPATS 15 instrument.

The crystallinity of the sheets obtained at different processing conditions was studied by means of differential scanning calorimetry (DSC) and x-ray analysis.

Small size samples (4mg) were heated from room temperature up to 250°C at 10°C/min in a Perkin Elmer DSC 7 calorimeter. The peak of the melting temperature range was taken as an indication of the average lamellar thickness of PP crystallites [7].

X-ray analysis was performed in a Philips PW 1729 instrument, ranging the 2θ angle from 6° to 36°. Being the glassy reinforcement amorphous, the crystalline fraction of each sample was determined as the ratio between the area of the peaks attributed to PP crystallites and the total area of x-ray patterns.

Results and discussion

The theory of linear viscoelasticity for polymers, like Hooke's law for elastic materials, is only a phenomelogical approximation of the real material performance. Strains outside the LVE range are considered critical for engineering applications, since the region of non linear viscoelasticity is very close to that of material failure [4]. According to the linear viscoelasticity theory, the response to an externally applied stress must satisfy both proportionality and superposition. For a linear viscoelastic material if different stresses, σ, are applied to the material at different times, the strain response, ε, is linearly proportional to the input stress, and the proportionality factor is a function of the elapsed time since the input stress. This is well expressed by the Boltzmann superposition integral for creep:

$$\varepsilon(t) = \int_0^t J(t-u)\frac{d\sigma(u)}{du}du \qquad \text{eq. (1)}$$

where J is a compliance function. The creep compliance consists of three components, i.e. elastic, viscoelastic and viscous. The elastic component is independent from time and temperature, whereas

the anelastic component, resulting from the sum of viscoelastic and plastic contributions, is dependent from both time and temperature. The anelastic compliance is also dependent from the applied stress in the non linear viscoelastic region [8]. The elastic component of the compliance is the reciprocal of the elastic modulus, which is different from the Young modulus determined from static tests, which also comprises viscoelastic effects.
In this work, the momentary anelastic creep compliance of the material was described with a three parameter fit model, first proposed for linear viscoelastic glass by Kohlrausch [9, 10]:

$$J(t) = J_0 \exp\left[\left(\frac{t}{\tau}\right)^m\right] \qquad \text{eq. (2)}$$

where τ is the temperature dependent relaxation time and J_0 and m are a characteristic compliance and a shape parameter not dependent from temperature. The dependence of compliance on the applied stress in the non linear viscoelastic region is accounted for using a stress dependent characteristic compliance J_0. By coupling eq. (1) and eq. (2) the strain resulting from an arbitrary load history can be expressed as:

$$\varepsilon(t) = \int_o^t \left(\frac{1}{E_0} + J_0 \exp\left[\left(\frac{t-u}{\tau}\right)^m\right]\right)\frac{d\sigma(u)}{du}du \qquad \text{eq. (3)}$$

When Eq(3) can fit the experimental with a constant value of J_0, the linear viscoelastic hypothesis is respected otherwise, in the non linear viscoelastic region, J_0 becomes a function of the stress.
Experimental deformation resulting from multiple load creep test for sample s130 at 30°C is reported in Figure 1. The load was ranged between 40 and 200MPa, corresponding to 14 and 70% of the ultimate load determined from static measurements. The line in Figure 1 is obtained applying a regression procedure on the experimental data using eq. (3). The calculated parameters are reported in Table I. A very good agreement is observed in Figure 1 between experimental data and Eq (3) predictions at the lower stresses. At the higher stress level the effect of non linearity is well evident since the measured deformation exceeds the deformation predicted by eq. (3) with a constant value of J_0.

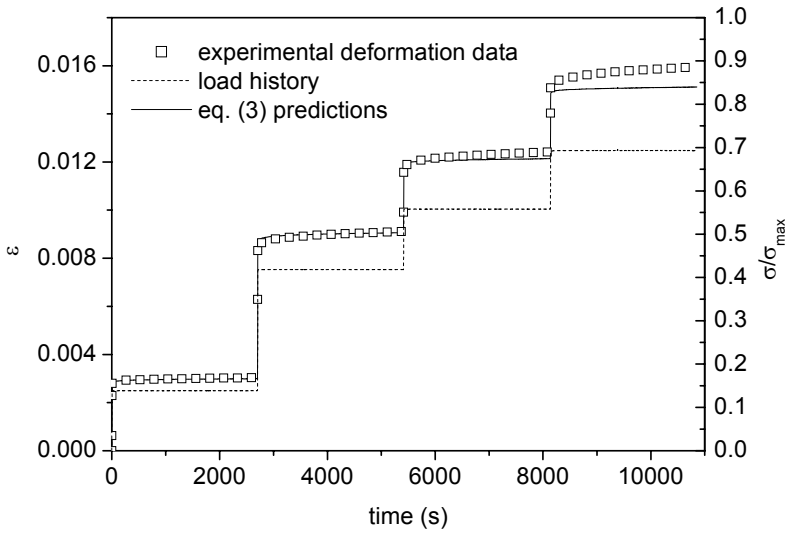

Figure 1: Multiple load creep test at 30°C: load history (- -), resulting experimental deformation (□) and eq. (3) prediction results (—)

Sample s130	E_0(MPa)	J_0 (MPa^{-1})	m	τ(s)
30°C	$4.87*10^5$	$3.58*10^{-5}$	0.0151	$1.52*10^{14}$
70°C	$4.87*10^5$	$3.58*10^{-5}$	0.0151	$1.41*10^{10}$
110°C	$4.87*10^5$	$3.58*10^{-5}$	0.0151	$1.37*10^7$

Table I: numerical values of fitting parameters of eq. (3) for multiple creep tests at 30, 70 and 110°C

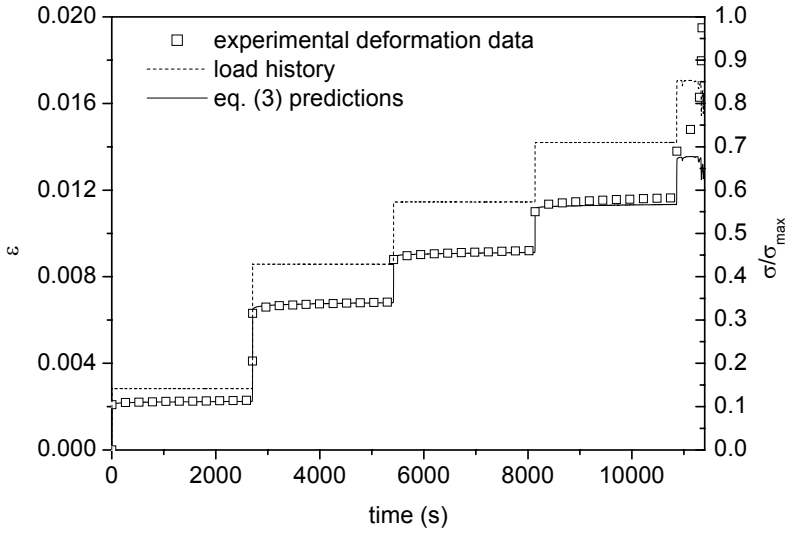

Figure 2: Multiple load creep test at 70°C: load history (- -), resulting experimental deformation (□) and eq. (3) prediction results (—)

In Figure 2 the multiple load creep test for sample s130 at 70°C is reported. The load was varied between 27 and 166 MPa, in the range between 14% and 84% of the ultimate load at 70°C. The regression curve of Figure 2 is obtained with same values of J_o, E_o and m used for Figure 1 and varying only τ. As shown in Table I, the value of τ decreases with temperature. At 70°C the creep behaviour of the material is linear for stresses as high as 108MPa, corresponding to 56% of the flexural strength at the same temperature. The behaviour becomes non linear for a stresses higher than 135MPa. In Figure 1 it was observed that the creep behaviour at 30°C becomes non linear when the stress exceeds a value of 120MPa, corresponding to 42% of the flexural strength. For the curve obtained at 110°C, where the load was varied between 14 and 83% of the ultimate strength, the sample showed a linear creep behaviour in the whole range of the applied stresses. Creep rupture was observed in the LVE region. The fitting parameters for the curve at 110°C are also reported in Table I.

This indicates that the linearity of creep is independent from the ratio of the applied load to the flexural strength. According to the observations reported in Figure 1 and Figure 2, the creep behaviour becomes non linear when the stress exceeds a threshold value. This value is a fraction of the ultimate strength that becomes higher increasing the temperature.

Non linear behaviour of polymeric materials is often attributed to damage formation at high values of the applied stress. However other factors can play a role in flexural creep of textile composites such as fiber alignment in tension and microbuckling in the compressed areas, damage at fiber intersection and finally debonding at the fibre-matrix interface [11].

In the linear viscoelastic region, for a 20MPa load, the effect of temperature on creep compliance was studied for the samples s80, s110 and s130. For the sample s80, the effect of temperature is shown in Figure 3.

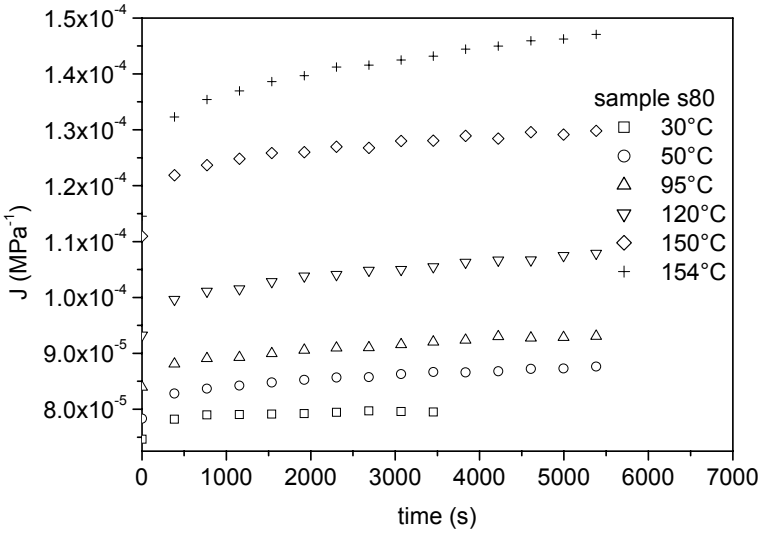

Figure 3: experimental creep compliance data for sample s80

As observed in Figure 3, the creep compliance of the laminate increases with increasing temperature, due to the increased free volume of the amorphous fraction of the polymer matrix. The effect is much higher at the higher temperatures, where some thinner crystals begins to melt, thus abruptly decreasing the stiffness of the material. The same behaviour can be observed in Figure 4 and Figure 5 for the curves obtained at different temperatures for samples s110 and s130.

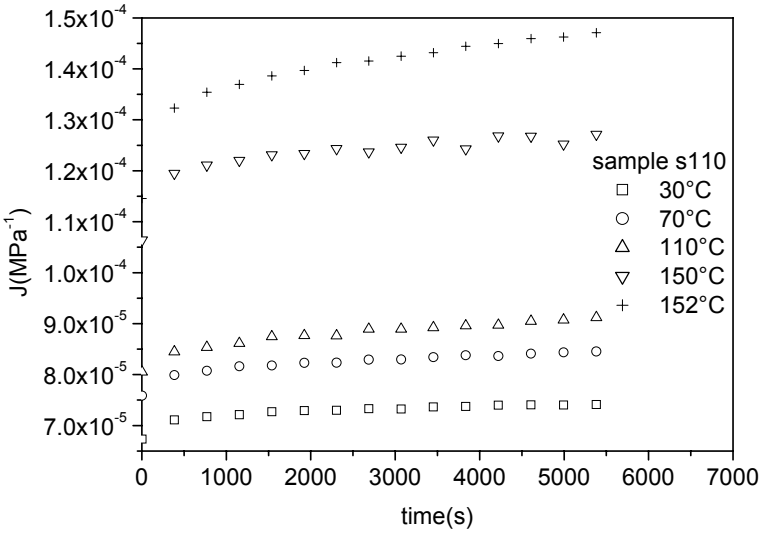

Figure 4: experimental creep compliance data for sample s110

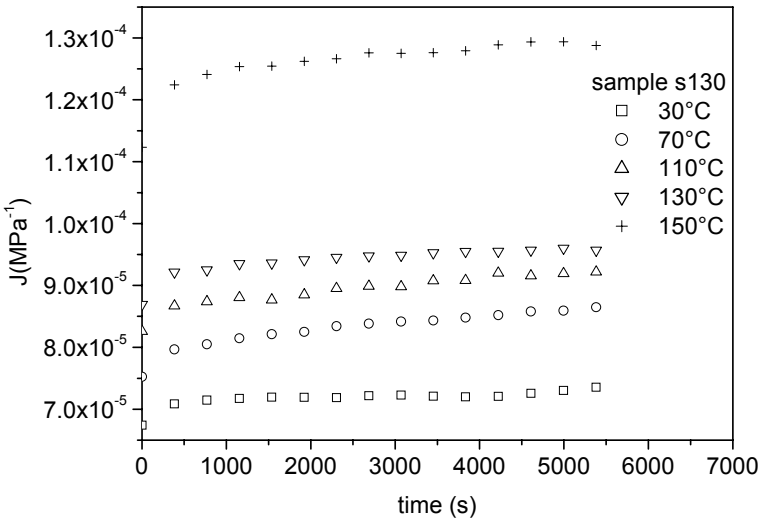

Figure 5: experimental creep compliance data for sample s130

Non linear curve fitting according to eq. (3) can be performed for the curves reported in Figure 3 through Figure 5. When multiple curve fitting is performed, the parameters of eq. (3) must be tied as to respect the time-temperature superposition principle. From time-temperature superposition principle, the compliance, $J(t_1)$, evaluated at time scale $t_1=t_0/a_T$ and temperature T_1 must be equal the compliance evaluated at time scale t_0, $J(t_0)$,and temperature T_0, where the subscript 0 denote the reference values:

$$\frac{1}{E_0(T_0)}+J_0(T_0)\exp\left[\left(\frac{t_0}{\tau(T_0)}\right)^{m(T_0)}\right]=\frac{1}{E_0(T_1)}+J_0(T_1)\exp\left[\left(\frac{t_0}{a_T\tau(T_1)}\right)^{m(T_1)}\right]\forall t \Leftrightarrow \begin{cases} E_0(T_0)=E_0(T_1) \\ J_0(T_1)=J_0(T_0) \\ m(T_1)=m(T_0) \\ \tau(T_1)=\dfrac{\tau(T_0)}{a_T} \end{cases} \quad \text{eq. (4)}$$

The values of E_0, J_0, m and τ can be found by non linear multiple curve fitting of eq. (3), with the conditions of eq. (4). Accordingly, for each temperature the value of the shift factor a_T can be determined from the last of eq. (4). Curves shifting on the time axis was performed to build the master curve at a reference temperature of 30°C for all the samples.

The shift parameters determined for different temperatures for sample s130 are reported in Figure 6. As it can be observed, the dependence from temperature of the shift factor cannot be explained with a WLF equation. This is a direct consequence of the very high values of compliance previously observed for the curves at the higher temperatures, where the polymer matrix approaches the viscous flow region [12]. Since the WLF equation usually applies for $T<T_g+100°C$, it was modified to account for an increase of the amorphous fraction occurring in the melting range:

$$\log(a_T)=\frac{-C_1(T-T_{ref})}{(C_2+T-T_{ref})(T_m-T)} \quad \text{eq. (5)}$$

where T_{ref} is the reference temperature for shifting (30°C in this work), T_m is the melting temperature of the polymer matrix, and C_1 and C_2 are two constants, dependent from the system under investigation. Non linear curve fitting of shift factor data according to eq. (5) is also reported in Figure 6, with the numerical parameters determined for the constants.

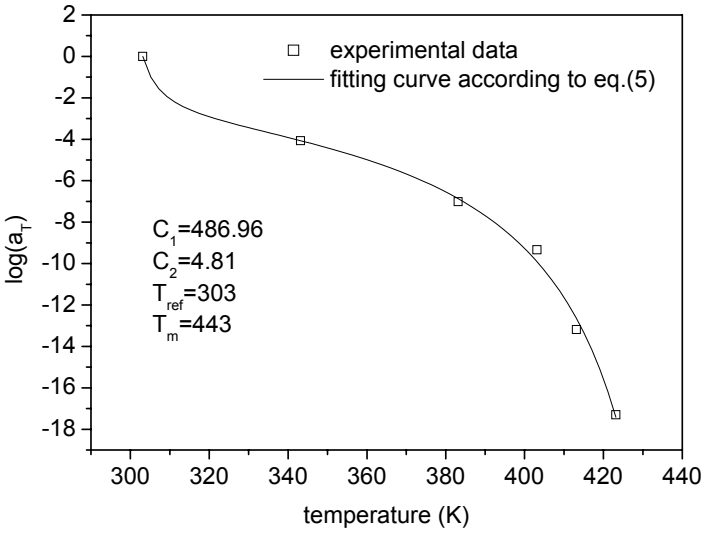

Figure 6: experimental shift factor data for sample s130 and non linear curve fitting from eq. (5)

The numerical values of the fitting parameters for eq. (3) are reported in Table II. The master curves for the samples s80, s110 and s130 are reported in Figure 7.

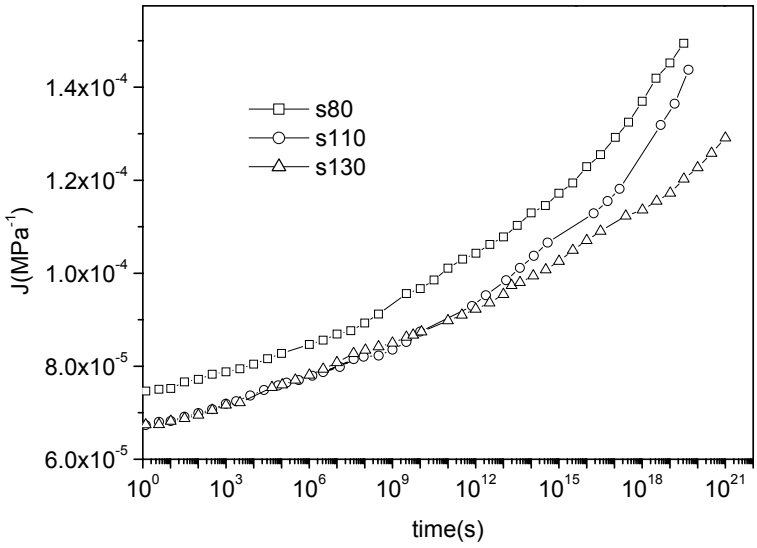

Figure 7: master curves at 30°C for samples s80, s110 and s130

	E_0(MPa)	J_0(MPa^{-1})	m	τ(30°C)(s)
s80	$4.87*10^5$	$3.89*10^{-5}$	0.0186	$1.12*10^{13}$
s110	$4.87*10^5$	$3.72*10^{-5}$	0.0196	$7.15*10^{13}$
s130	$4.87*10^5$	$3.58*10^{-5}$	0.0151	$1.52*10^{14}$

Table II: numerical values of the fitting parameters for eq. (3) for samples s80, s110 and s130 at 20MPa

For the three curves reported, the laminate shows the typical rubbery region, (the glass transition of the polymer is lower than room temperature) and viscous flow, where the polymer behaves like a highly viscous melt. A decrease of the creep compliance is observed as moulding temperatures increases, indicating that the creep behaviour of the material is dependent from the structure of the polymer matrix and the process conditions. This is reflected in lower values of the initial creep

compliance J_0, and in higher relaxation times when moulding temperature increases, as observed from the values of the parameters reported in Table II. The differences between the samples moulded at 110 °C and 130 °C are evident only at very long times indicating that these two processing temperatures are substantially equivalent for their effects on the of the composite.
As a consequence of the differences observed in the creep behaviour of the Twintex laminates obtained under different processing conditions, the crystalline structure of the polymer matrix was studied using DSC analysis. The melting peak was regarded as an indication of average lamellar thickness of polymer crystallites [7, 13]. The DSC melting peak temperatures for samples s80, s110 and s130 reported in Table III show that increasing moulding temperature thicker crystallites are obtained in the polymer matrix.
Also, the crystalline fraction of the composite was determined from X-ray analysis. X-ray diffraction patterns for samples s80, s110 and s130 are reported in Figure 8 in the range between 2θ=12° and 2θ=20°. The same diffraction patterns are reported in Figure 9 in the range between 2θ=20° and 2θ=30°.

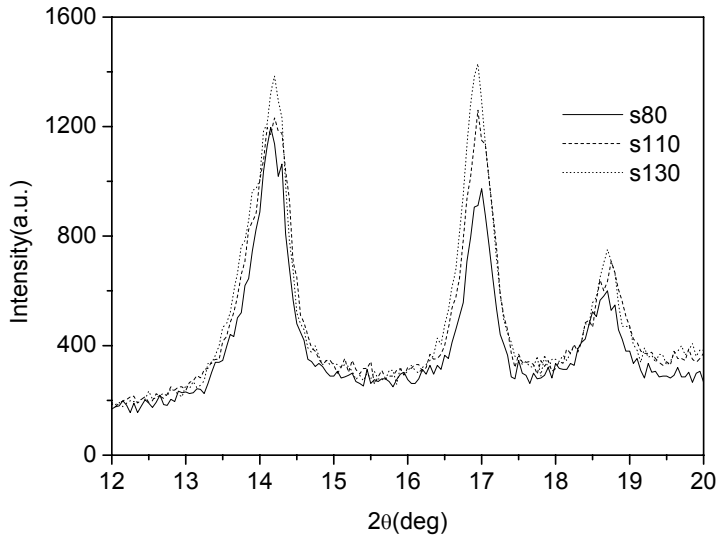

Figure 8: x-ray patterns for samples s80, s110 and s130 in the range between 2θ=12° and 2θ=20°

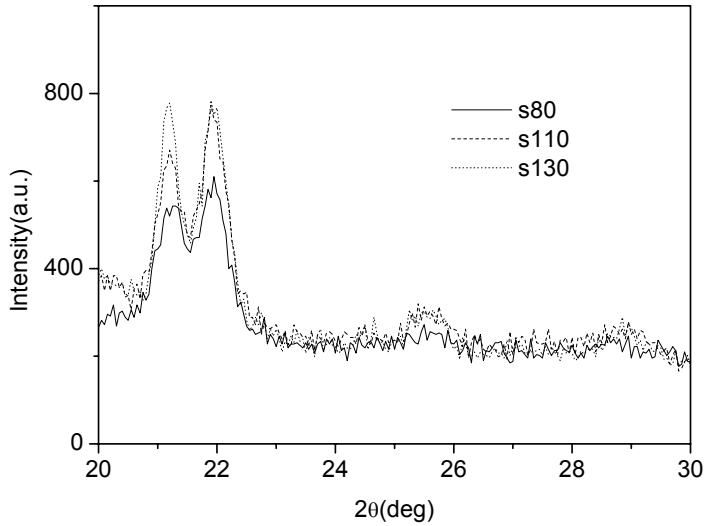

Figure 9. x-ray patterns for samples s80, s110 and s130 in the range between 2θ=20° and 2θ=30°

In both figures, representing the scattered intensity as a function of scattering angle, the characteristic reflection angles of PP crystalline structures can be used to study the crystalline morphology of the polymer. The amorphous fraction of material is responsible of the background intensity, whereas the crystalline fraction is responsible of the observed peaks. The contribution of the glassy reinforcement to crystalline peaks was considered to be absent, since the reinforcing material is a completely amorphous phase.
From the results of Figure 8 and Figure 9 it can be observed that the position of the characteristic peaks is not influenced from the processing conditions. The peaks at $2\theta=14.5°$, $2\theta=17°$, $2\theta=18.6°$, $2\theta=21.2°$ and $2\theta=21.9°$ are characteristic of a monoclinic α-PP unit cell [14]. The α form is the most common crystalline phase of isotactic polypropylene (iPP), observed for both melt and solution crystallized samples prepared at atmospheric pressure. Other crystalline forms of iPP (hexagonal β and orthorhombic γ) are less common, and can be obtained under controlled crystallization conditions [15].
The crystalline fraction in each sample was determined as the ratio between the area of the characteristic peaks of iPP crystallites and the total area of x-ray patterns [13]. If no crystalline phase is present in the glassy reinforcement, the ratio calculated is an indication of iPP crystallinity. From the diffraction patterns reported in Figure 8 and Figure 9, the crystalline fractions reported in Table III was determined. The higher crystalline fraction obtained increasing the press plates temperature corresponds to lower undercooling and to the growth of larger lamellae and spherulites, as also confirmed by the DSC melting peaks.
The viscoelastic response of semicrystalline polymers is conventionally associated with rearrangement of chains in amorphous regions. Sliding of tie chains along and their detachment from lamellae play the key role in the time-dependent response of semicrystalline polymers [16]. With increasing moulding temperature, higher degree of cristallinity and increased average lamellar thickness of polymer crystallites improves the stiffness of the laminate composite. On the other hand, increased cristallinity usually reduces tenacity of the composite.
For the three samples Charpy impact tests results are reported in Figure 10 and in Table III. As it can be observed, the impact resistance of the laminate decreases with increasing moulding temperature, as a consequence of lamellar thickening.

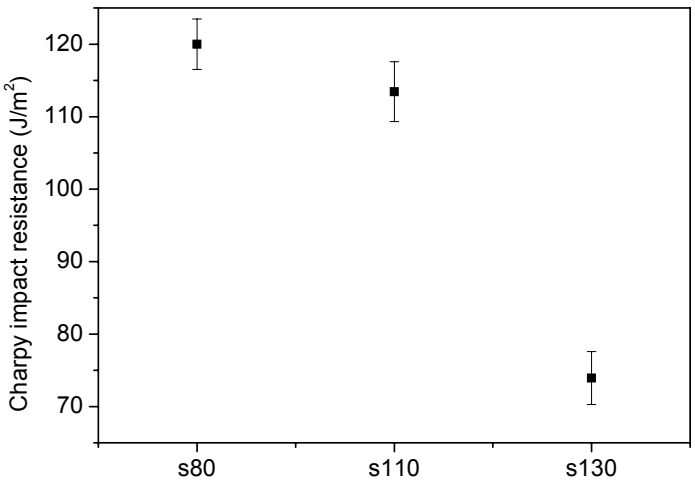

Figure 10: Charpy impact resistance data for samples s80, s110 and s130

Sample	Degree of cristallinity (x-ray)	Charpy Impact resistance (J/m^2)	DSC melting peak (°C)
s80	0.33	120±3.47	159.1
s110	0.35	113.45±4.13	159.4
s130	0.46	73.93±3.65	160.2

Table III: degree of crystallinity, Charpy impact resistance and DSC melting peak for samples s80, s110 and s130

Conclusions

Flexural creep behaviour of commercially available thermoplastic matrix composite was presented. The stress limits of linear viscoelastic (LVE) behaviour were determined at about 55% of the ultimate flexural stress and can depend from the complex interaction between fibers and matrix and to fiber misalignment. In the LVE region, time- temperature superposition principle was successfully applied to build creep master curves, predicting the mechanical behaviour of the composite at long time scales and a single reference temperature. For the PP based composite, the typical rubbery and viscous flow regions can be observed. Furthermore the creep behaviour of the composite was related to the matrix crystallinity, depending from the processing conditions. In particular increasing the moulding temperature, a higher degree of crystallinity and average lamellar thickness has been found in the polymer matrix. This has been evidenced through x-ray and DSC analysis. Even though, a higher crystallinity and larger crystallites can improve the creep resistance of the composite, they can also reduces its toughness, as evidenced by the decreased Charpy impact resistance.

Acknowledgment:

CETMA consortium is kindly acknowledged for financial support in the framework of project MAVET. Special thanks to Ing. Luigi Barone, Ing Orazio Manni and Ing. Alessandra Passaro for the useful discussion.

References

1 Pegoretti,A. Ricco,T. *Journal of Materials Science*, 36, (2001), 4637–4641
2 Ren,W. *Materials Science and Engineering*, A334, (2002), 312-319
3 Nicholson,L.M. Whitley,K.S. Gates,T.S. *Mechanics of Time-Dependent Materials,* 5, (2001), 199–227
4 Wortmann,F.J. Schulz,K.V. *Polymer*, 36, (1995), 2363-2369
5 Keating,M.Y. Malone,L.B. Saunders,W.D. *Journal of Thermal Analysis and Calorimetry*, 69, (2002), 37–52
6 ASTM D 2990-95 Standard Methods for Tensile, Compressive and Flexural Creep and Creep Rupture of Plastics
7 Greco,A . Maffezzoli,A. *Journal of Applied Polymer Science*, 89, (2003), 289-295,
8 Boey,F.Y.C Lee,T.H. Khor,K.A. *Polymer Testing*, 14, (1995), 425-438
9 Kohlrausch, R., Annals of Physiscs, **72,** 393-425, (1847).
10 Tomlins,P.E. *Polymer*, 37, (1996), 3907-3913
11 Gregory,A. et al. *Mechanics of Time-Dependent Materials,* 3, (1999), 71-84
12 Tobolsky,A.V. *Properties and Structure of Polymers* Wiley, New York, (1960)
13 Wunderlich,B. Macromolecular Physics, Vol. 1, Academic Press, New York (1976)
14 Dean,D.M. Rebenfeld,L. Register,R.A. Hsiao,B.S. *Journal of Materials Science*, 33, (1998), 4797-4812
15 Krumova,M. Karger-Kocsis,J. Balt,F.J. Calleja,A. Fakirov,S. *Journal of Materials Science*, 34, (1999), 2371-2375
16 Drozdov,A.D. deClaville Christiansen,J. *Polymer,* 43, (2002), 4745-4761